Extended Abstracts of the 2020 International Conference on Solid State Devices and Materials, VIRTUAL conference, 2020, pp507-508

Evaluation of hexagonal boron nitride crystals in terms of an insulating building block of van der Waals heterostructures

Momoko Onodera[1], Kenji Watanabe[2], Miyako Isayama[1], Satoru Masubuchi[1], Rai Moriya[1], Takashi Taniguchi[3,1], and Tomoki Machida[1]

[1] Institute of Industrial Science, Univ. of Tokyo
4-6-1, Komaba, Meguro-ku, Tokyo 153-8505, Japan
Phone: +81-3-5452-6158 E-mail: monodera@iis.u-tokyo.ac.jp
[2] Research Center for Functional Materials, National Institute for Materials Science
1-1 Namiki, Tsukuba 305-0044, Japan
[3] International Center for Materials Nanoarchitectonics, National Institute for Materials Science
1-1 Namiki, Tsukuba 305-0044, Japan

Abstract

Hexagonal boron nitride (h-BN) is an insulating layered material having a bandgap of ~6 eV. It is the only insulating 2D material and used as an atomically flat insulating substrate for all sorts of layered materials, playing an essential role in 2D materials research. In this work, we investigate the quality of h-BN single crystals from the viewpoint of its application to van der Waals heterostructures. We probe the quality of h-BN by attaching graphene as a probe material and investigating carrier transport of graphene/h-BN.

1. Carbon-rich domain in HPHT h-BN

h-BN crystals synthesized under high pressure and high temperature (HPHT) are known to have high quality. HPHT h-BN has been an essential component of van der Waals (vdW) heterostructures and used as an insulating bottom substrate, thin tunneling barrier, and potential modulator. Today, HPHT h-BN is used in more than 200 research institutes worldwide. However, we found that all HPHT h-BN crystals have a distinct carbon (C)-rich domain at the core region, which contains a significant amount of C impurities. Figures 1a,b show a scanning electron microscope (SEM) image and cathodoluminescence (CL) image of an HPHT h-BN crystal, respectively. Although the crystal seems uniform in the SEM image, it is separated into two distinct regions in the CL image. The central region of the crystal, which we call the 'domain', has significantly high concentration of carbon impurities (3×10^{18} –1×10^{19} cm^{-3}), confirmed by the secondary ion mass spectroscopy (SIMS). In the spherical region of the crystal, which we call 'pristine' region, the carbon density is under the detection limit (<10^{18} cm^{-3}).

Figures 1c,d show an optical micrograph and photoluminescence (PL) image at a wavelength of 340 nm, respectively, of an exfoliated HPHT h-BN flake on a SiO_2/Si substrate. Importantly, this domain still exists after exfoliation and cannot be identified with an optical microscope or atomic force microscope (AFM). Therefore, the existence of the domain has not been recognized so far. Considering the worldwide use of HPHT h-BN in the field of 2D materials, it is urgently demanded to investigate the influence of the domain in vdW junctions.

To evaluate the influence of the C-rich domain on the adjacent graphene, we fabricated graphene/h-BN heterostructures with graphene placed across the boundary of the domain, which enabled us to measure graphene on the domain and pristine regions simultaneously (Figures 1e,f). To detect the C-rich domain in HPHT h-BN flakes, we utilized photoluminescence in ultraviolet (UV) range, which does not contaminate the flake during the measurements. At low temperatures, we measured the transport properties of graphene and found that graphene on the C-rich domain exhibited degraded carrier mobility than that on the pristine region (Figures 1g,h). When applying a perpendicular magnetic field, graphene on the C-rich domain exhibited characteristic bending in the Landau fan diagram (Figure 1i). These results indicate that the C-rich domain imposes a negative influence on the adjacent graphene [1].

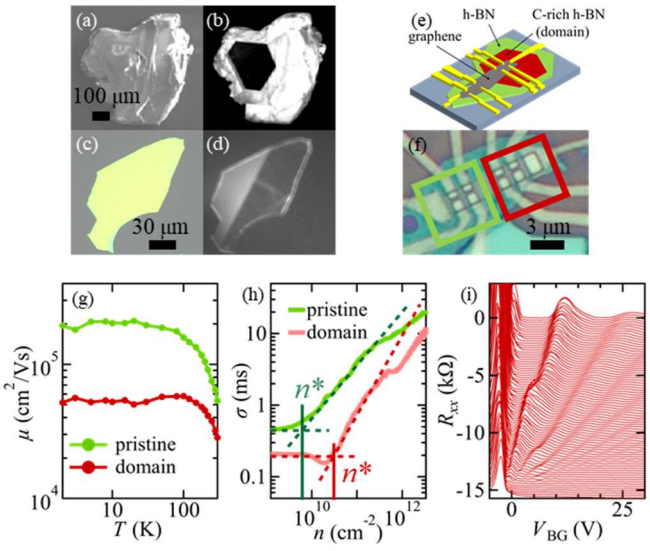

Fig. 1 (a) SEM and (b) CL (320 nm) images of an HPHT h-BN crystal. (c) Optical microscope and (d) PL (340 nm) images of an exfoliated HPHT h-BN flake. (e) Schematic and (f) photographic image of the device. (g) Temperature dependence of carrier mobility. (h) Extraction of charrier inhomogeneity n^* at T = 2 K. (i) R_{xx} vs. V_{BG} at B = 0-9 T obtained in graphene on the C-rich domain. Data are offset in proportional to B for clarity.

2. Carbon-doped HPHT h-BN

As discussed in the last section, the C-rich domain in HPHT h-BN distorts the transport properties of the adjacent graphene. To further investigate the role of carbon impurities in h-BN, we conducted experiments using intentionally carbon-doped HPHT h-BN (C-doped h-BN) [1].

Graphene on C-doped h-BN shows anomalous bending in the Landau fan diagram (Figures 2a-d). To precisely estimate the energy where the bending occurs, we first derived the Fermi velocity v_F in graphene on C-doped h-BN by cyclotron resonance measurements (Figure 2e). Then, using the derived v_F value, we plotted the bending energy E_{bend} and obtained $E_{bend} \sim 90$ meV above the Dirac point. Other samples showed the similar trend (Figure 2g). The bending in the Landau fan diagram suggests the formation of impurity levels at E_{bend}. To further confirm the existence of an impurity level, we measured the hysteresis of the longitudinal resistance R_{xx}. The hysteresis started to appear when the Fermi energy cross over E_{bend}. This observation supports the formation of an acceptor level.

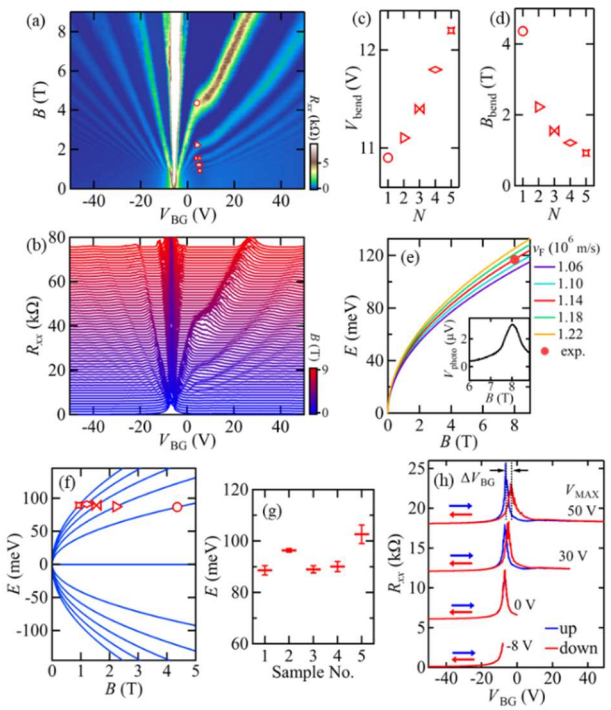

Fig. 2(a) Colormap of R_{xx} as a function of V_{BG} and B at T = 1.6 K. (b) R_{xx}–V_{BG} plots in the range of B = 0–9 T. Data are offset, in proportion to B, for clarity. (c) V_{bend} and (d) B_{bend} as functions of N. V_{bend} is expressed relative to the DP. (e) LL transition energy for $N = 0 \rightarrow 1$ calculated with different v_F values (solid lines). The red circle indicates the value corresponding to the CR experiment result (E_{photo} = 116.84 meV, B_{CR} = 8.02 T); this is plotted as V_{photo} versus B at the DP (inset). (f) E_{bend} as a function of B for different values of N. The blue lines indicate the LLs of monolayer graphene calculated using the experimentally-derived value $v_F = 1.14 \times 10^6$ m/s. (g) E_{bend} for five samples of graphene on C-doped h-BN and graphene on a C-rich domain of HPHT h-BN. (h) V_{BG}–R_{xx} plots for different sweep ranges. The plots are offset vertically for clarity.

3. h-BN crystals synthesized under atmospheric pressure

All HPHT h-BN crystals inevitably have the C-rich domain, which distorts the transport of the adjacent graphene. Then, how can we avoid the use of the C-rich domain? One of the choices is to use h-BN crystals that do not have any impurity-rich domain.

We found that h-BN crystals synthesized under atmospheric pressure and high temperature (APHT) can be used without the concern of the impurity-rich domain. CL images of APHT h-BN crystals do not exhibit distinct domains (Figures 3a-c). To test the quality of APTH h-BN as a substrate for 2D materials, we fabricated graphene devices sandwiched by APHT h-BN (Figure 3d). At low temperatures, R_{xx} showed a sharp peak at the charge neutrality point (Figure 3e). The charge inhomogeneity n^* and the carrier mobility μ are estimated as $n^* \sim 1.6 \times 10^9$ cm^{-2} and $\mu \sim$ 1,000,000 cm^2/Vs at T = 1.6 K, which is comparable or even lower than that in high-quality graphene sandwiched in HPHT h-BN (Figures 3f,g). These results demonstrate that APHT can be used as high-quality insulating substrate for graphene which is comparable to HPHT h-BN [2].

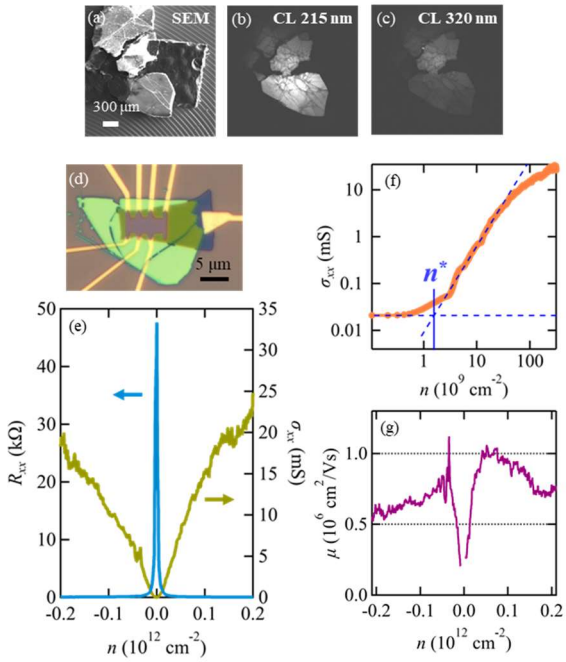

Fig. 3(a) SEM image, (b) CL images at wavelengths of (b) 215 nm and (c) 320 nm of an APHT crystal grown by a solvent of Co-Cr. (d) Optical image of the device. (e) R_{xx} (blue) and σ_{xx} (yellow) as a function of n at T = 1.6 K. (f) σ_{xx} as a function of n at T = 1.6 K in a double-logarithmic scale. The dotted lines show the extraction of n^*. (g) Carrier mobility μ as a function of n.

References

[1] M. Onodera, K. Watanabe, M. Isayama, M. Arai, S. Masubuchi, R. Moriya, T. Taniguchi, and T. Machida, Nano Lett. **19**, 7282 (2019).

[2] M. Onodera, M. Isayama, T. Taniguchi, K. Watanabe, S. Masubuchi, R. Moriya, T. Haga, Y. Fujimoto, S. Saito, and T. Machida, Carbon. **167**, 785 (2020).

[3] M. Onodera, T. Taniguchi, K. Watanabe, M. Isayama, S. Masubuchi, R. Moriya, and T. Machida, Nano Lett. **20**, 735 (2020).